Available online at www.sciencedirect.com

ScienceDirect

Transportation Research Procedia 38 (2019) 524–543

Transportation Research Procedia

www.elsevier.com/locate/procedia

23rd International Symposium on Transportation and Traffic Theory, ISTTT 23, 24-26 July 2019, Lausanne, Switzerland

Modeling double time-scale travel time processes with application to assessing the resilience of transportation systems

R.X. Zhong[a,d], X.X. Xie[a], J.C. Luo[b], T.L. Pan[c], W.H.K. Lam[d], A. Sumalee[d,*]

[a]*Guangdong Key Laboratory of Intelligent Transportation Systems, School of Intelligent Systems Engineering, Sun Yat-Sen University, Guangzhou, China*

[b]*Shenzhen Urban Transport Planning Center, Shenzhen, China*

[c]*Research Institute for Smart Cities, School of Architecture and Urban Planning, Shenzhen University, Shenzhen, China*

[d]*Department of Civil and Environmental Engineering, The Hong Kong Polytechnic University, Hong Kong SAR, China*

Abstract

This paper proposes a double time-scale model to capture the day-to-day evolution along with the within-day variability of travel time. The proposed model can be used to evaluate short-term to long-term effects of new transport policies and construction of critical infrastructures, and to analyze the resilience of road networks under disruptions. The within-day travel time variability is modeled using the functional data analysis, in which the effects of road traffic congestion and noise of traffic data are considered explicitly. The within-day process is then regarded as the local volatility (or the noise process) to drive the day-to-day process while the latter is described by a modified geometric Brownian motion (GBM). Then, the day-to-day travel time process is obtained by the statistics of the modified GBM. The model probabilistically captures the evolution of day-to-day and within-day travel time processes analytically. Moreover, an efficient method based on the cross-entropy method is developed for calibrating the model parameters. A lasso-like regularization is employed to guarantee a small bias between the model estimations and the measurement counterparts. Finally, two empirical studies are carried out to validate the proposed model at different scales with different traffic scenarios, i.e., a case study on the Guangzhou Airport Expressway (link to path scale) under traffic accident conditions and a case study in New York City (city-scale) to analyze the network resilience under Hurricane Sandy. Both case studies adopted probe vehicle data but with different configurations (fine versus coarse, small versus big data). The empirical studies confirm that the proposed model can accommodate the inherent variability in traffic conditions and data meanwhile being computationally tractable. The numerical results illustrate the applicability of the proposed model as a powerful tool in practice for analyzing the short-term and long-term impacts of disruptions and systematic changes in the performance of road networks.

Peer-review under responsibility of the scientific committee of the 23rd International Symposium on Transportation and Traffic Theory.

Keywords: Double time-scale dynamics; day-to-day; within-day; dynamic travel time distribution; traffic network resilience.

* Corresponding author

E-mail addresses: zhrenxin@mail.sysu.edu.cn (R.X. Zhong)., cehklam@polyu.edu.hk (W.H.K. Lam)., ceasumal@polyu.edu.hk (A. Sumalee).

2352-1465
Peer-review under responsibility of the scientific committee of the 23rd International Symposium on Transportation and Traffic Theory.
10.1016/j.trpro.2019.05.028

1. Introduction

The steady-state equilibrium paradigm was adopted as the basis for predicting the impacts of transport measures for decades. However, transportation systems do not always operate at steady state but suffer from a range of intrinsic and exogenous factors, such as daily demand fluctuations, special social events, adverse weather conditions, traffic accidents, road maintenance works, and new transport policies. These uncertainties may cause irregular transportation system disruptions and degradations while making the network vulnerable and lead to dynamic variability of traffic flow patterns and travel costs. The dynamic traffic assignment (DTA) focusing on the within-day traffic dynamic extensions of the equilibrium paradigm implicitly assumes the between-day scale to be constant, or the day-to-day variation of the general pattern of traffic, especially the travel demand pattern, is not significant, see, e.g., Friesz et al. (1993); Chow (2009); Zhong et al. (2011, 2012). The static assumption of the day-to-day traffic pattern limits the within-day models to take into account the between-day variation of travel demand and other exogenous factors induced by the ever-changing external environment, e.g., demand variation and supply disturbances (Cantarella and Watling, 2016).

On the other hand, a growing body of day-to-day dynamics research assumes the traffic in the within-day scale is static while it is dynamic in the between-day scale. The day-to-day dynamics refers to the evolution of traffic between successive reference periods (the whole day or part of it, e.g., the morning peak period), see, e.g. Smith (1984); Friesz et al. (1994, 1996); Nagurney and Zhang (1997); Sandholm (2010); He et al. (2010); He and Liu (2012); Guo et al. (2015) in the deterministic setting; Cascetta and Cantarella (1991); Cantarella and Watling (2016) in the stochastic setting. The within-day static traffic assumption enables the day-to-day models analytically tractable at the price of losing important characteristics of congestion and thus decreasing the accuracy of the day-to-day models. However, it is known that transportation systems are not memory-less. For example, travel time is a consequence of travelers' route and departure time choices subject to the stochastic network supply (e.g., disruptions). Initial states of the system will affect the actual travel time under the same demand/flow. Real-time information/prediction of within-day dynamics could affect the travelers' decisions on departure time and route choice (which yields the within-day dynamic traffic) and thus influence travelers' trip-to-trip learning which results in day-to-day evolutions of network flow pattern and travel time (Guo et al., 2018).

To capture the interaction between the within-day and day-to-day scales and to remedy the drawbacks of the above individual approach, several recent studies, e.g., Friesz et al. (2011); Liu et al. (2017); Liu and Geroliminis (2017); Guo et al. (2018), have made efforts in developing double time-scale dynamic traffic models. However, all these models rely on simplified deterministic (within-day) traffic flow models. Nevertheless, these models involve plenty of model parameters and are not ready for model calibration and validation from field traffic data. Developing a double time-scale dynamic model that can be calibrated, validated and driven by real-world traffic data is an emerging task. Moreover, it is also necessary to incorporate the uncertainties and noise in traffic data in the double time-scale dynamic traffic model. These will enable us to deal with many aspects of both dynamic change and uncertainty/variability while representing the time evolution as a stochastic process driven by real-time traffic data.

Most of the existing day-to-day, within-day, and double time-scale dynamic models (if not all) use flow measures (Crawford et al., 2017). On the other hand, travel time is a standard measure for evaluating the performance of transportation systems. Modeling dynamic travel time plays a vital role in travelers' information systems, traffic control and management. In the literature, travel time is also a direct measure for assessing the network reliability/vulnerability. An extensive amount of literature devised risk measures to evaluate the variability in travel time based on within-day travel time estimates. However, little attention is paid to investigate the day-to-day travel time evolution. Therefore, it is of great significance to consider the travel time variability within a day when evaluating the day-to-day traffic conditions. In this study, we first propose a double time-scale travel time model to consider the day-to-day and within-day travel time evolution under uncertainties.

Characterizing travel time variability by the statistical properties provides a powerful means for understanding its reliability and quantifying traffic network performance. State-of-art practice often adopts the mean and variance of travel time to define its reliability and to develop indices such as the Buffer Time and Planning Time based on the Gaussian assumption of travel time distribution. However, empirical studies have shown that travel time distributions were not symmetrical but with high skewness and heavy tails especially under traffic disruptions such as accidents and adverse weather conditions (Kim and Mahmassani, 2015; Sumalee et al., 2013). These common indices may not

be informative for assessing the heavily skewed distributions (Kim, 2014). To this end, various probability distributions have been proposed to model the variability of travel time, and the suggestions of these models under different circumstances have been discussed. Some most widely used distributions are the Log-normal, Gamma and Weibull distributions (Fosgerau and Fukuda, 2012; Taylor, 2013; Kim and Mahmassani, 2015). Al-Deek and Emam (2006) analyzed the loop detector data to investigate four kinds of distributions, i.e., Lognormal, Weibull, Normal and Exponential. It was found that the Lognormal distribution best fits the travel time distribution. Kim and Mahmassani (2015) proposed a compound Gamma representation for modeling both the within-day (or vehicle-to-vehicle) and day-to-day travel time variability under the linearity assumption of the relationship between mean and standard deviation. However, Yildirimoglu et al. (2015) commented that this relationship could not be captured by a linear curve in the day-to-day time-scale. Nevertheless, most of the risk measures do not capture the effect of the heavy tails in dynamic travel time distributions induced by rare extreme traffic events. It is important to understand the transportation system performance in terms of risk for the total system cost to develop control strategies for risk management in traffic network under uncertainties. In terms of risks, vulnerability analysis could be connected with the reliability analysis of travel time distributions with heavy tails. Thus, we introduce a double time-scale risk measure for characterizing travel time variability and identifying the most vulnerable links (or regions).

This study addresses the need of double time-scale (within-day and day-to-day) travel time model to describe the overall travel time variability, which allows evaluating the short-term to long-term impacts of traffic disruptions and systematic changes on the performance of traffic networks. Firstly, the within-day travel time variability that captures the effects of traffic congestion and noise in traffic data is established via functional data analysis (FDA) (Guardiola et al., 2014; Wang et al., 2016; Crawford et al., 2017; Zhong et al., 2017). The FDA is used as a data filtering tool and a dictionary-based data compression method to identify travel time features of both spatial and temporal dimensions. To this end, the within-day process can be regarded as a data-driven component of the proposed model that enables the model to take in the raw traffic data with dynamic and noisy nature, which is unlike the conventional day-to-day models. Secondly, the day-to-day travel time process is modeled via a discretized version of a modified Geometric Brownian Motion (GBM) by incorporating the within-day process as local volatility to yield a double time-scale model. Given the statistics of the within-day travel time process, analytic results that probabilistically capture the evolution of day-to-day travel time process are derived. The modified GBM can be regarded as a model-driven component of the proposed model. *In this sense the proposed double time-scale travel time model can be viewed as an integration of data-driven and model-driven approaches.*

Similar to Watling and Hazelton (2018), the proposed double time-scale travel time model can describe the variability of the day-to-day evolution from the transient impact to the steady-state behavior (if any) of some systematic changes in traffic network, e.g., bridge collapse, hurricane, and new traffic policy measures. Meanwhile, the proposed model can capture the variability of within-day travel time process and the effect of noise in traffic data. To our best knowledge, conventional dynamic evolution models are often built on traffic assignment models and without model calibration using real traffic data. For example, conventional day-to-day models **cannot** take in raw traffic data with dynamic and noisy nature directly but have to aggregate the raw traffic data collected within a day into a "point" because of the within-day static traffic assumption. This data preprocessing requires an expert level of experience and causes bias to the conventional day-to-day models while inducing difficulty in model calibration with traffic data apart from the behavior realism. In this respect, a relative entropy-based (also known as Kullback-Leibler (KL) distance) method is proposed for calibrating the proposed double time-scale travel time model, leading to proper distributions of interest. Finally, we apply the double time-scale travel time model for resilience analysis by introducing a risk-based measure that adapts the heavy-tailed travel time distributions to quantify the deterioration of network performance. For a better grasp and understanding of this paper, a precedence diagram for the proposed double time-scale dynamic travel time model and its application on network resilience analysis is depicted in Figure 1.

The rest of this paper is organized as follows. Section 2 presents the derivation of the double time-scale travel time processes. Section 3 proposes a model calibration scheme for the proposed double time-scale travel time model. Two empirical studies are conducted in Section 4 to validate the proposed model at different scales under different traffic scenarios. Application of the proposed model for the resilience analysis is also discussed in the empirical studies. Finally, Section 5 concludes the paper. Companion materials and proofs are provided in the online appendix at `https://www.dropbox.com/sh/ul6df71pg3pggbc/AABVwKZHHYKBVSkF_9PKgnBPa?dl=0`. At the end of this section, we summarize the key notations throughout this paper in Table 1.

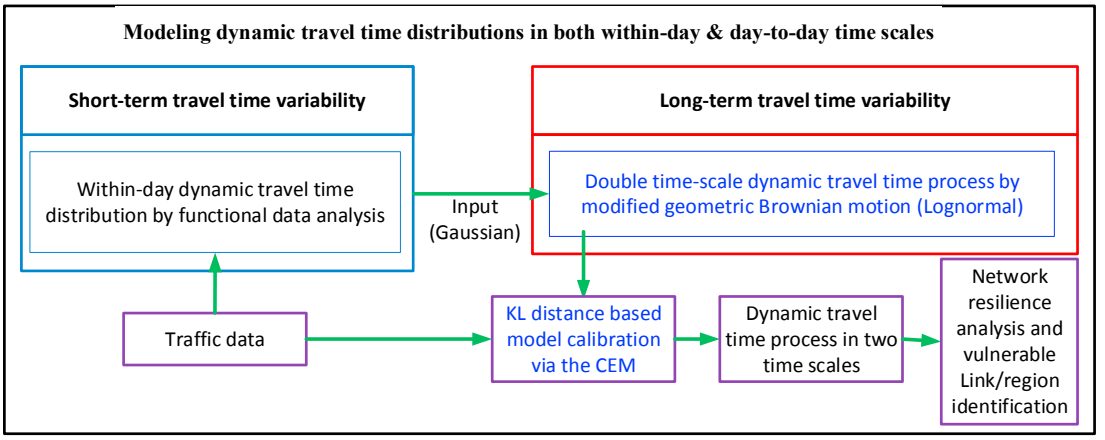

Fig. 1. Framework for modeling the double time-scale dynamic travel time variability.

Table 1: List of notations.

Notations	Descriptions
T_m	Discretized time interval within one day, $m = 1, \cdots, M$
$\mathbf{V_m}$	A matrix of travel time samplings
$\mathbf{W_m}$	A vector of daily realizations
$X_m(i)$	Day-to-day travel time process at time slot m where days are indexed by $i = 1, \cdots, N$
X_{im}	Within-day travel time process of day i at time interval T_m
n_i	The number of data samples collected in day i
e_{im}	The noise term under independent identically Gaussian distribution
t, s	Time variable
$\mu(t)$	Mean function of travel time
λ_k	Eigenvalue from the orthonormal expansions of the covariance function of travel time
$\psi_k(t)$	Eigenfunctions from the orthonormal expansions of the covariance function of travel time subject to orthonormal constraints, i.e. $\int_{T_m} \psi_k^2(s)ds = 1$ and $\int_{T_m} \psi_y(s)\psi_k(s)ds = 0, \forall y < k$
ξ_{ik}	Scores of principal components
κ	The accuracy level
μ_{im}, σ_{im}	The mean and standard deviation of travel time function of day i during time interval T_m
ϵ	Standard Gaussian distribution, i.e. $\mathbb{N}(0, 1)$
α_m	Drift parameter of stochastic process X_m
β_m	Volatility parameter of stochastic process X_m
$\Delta F_m(i)$	A discrete stochastic process
$E[\Delta F_m(i)]$	The mean of $\Delta F_m(i)$
$D[\Delta F_m(i)]$	The variance of $\Delta F_m(i)$
δ	Width of the bounding box
ϕ_1, ϕ_2	Sample size for the random sampling and importance sampling
U	Parameter set
$R_m(i)$	Network-scale pace distribution
d	The trip type, $d = 1, \cdots, D$
$X_m^d(i)$	The pace distribution of trip type d at time interval T_m in day i
a^d	Importance weighting of trip type d

2. Modeling dynamic travel time distributions in both within-day & day-to-day time-scales

The dynamic travel time variability is defined from two perspectives: (1) the day-to-day travel time variability that concerns the travel time variation over different days along a particular route at a given departure time interval; and

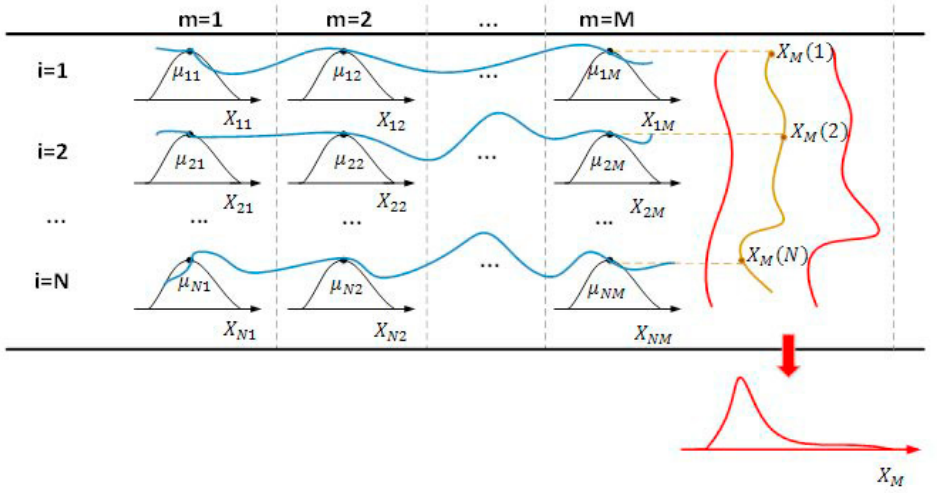

Fig. 2. An illustration of dynamic travel time processes and distributions. The blue curves are realizations of X_{im} (the within-day process of day i) and yellow curves are realizations of $X_m(i)$ (the day-to-day process observed during time interval T_m, e.g., $8:00-8:05$ AM), while the red curves depict the confidence interval of $X_m(i)$. The mean process of the double time-scale travel time model and its confidence intervals can be described by a three-dimensional image as it will be shown in the empirical studies.

(2) the within-day travel time variability that refers to the travel time experienced by different drivers who depart within the same time slot or the dynamics of travel time with respect to different departure time. Figure 2 illustrates the definition and relationship of travel time in double time-scales. Within-day travel time process is denoted by $X_i(t)$ for day $i = 1, \cdots, N$ where t denotes the (within-day) time instant. Raw traffic data collected every day may be with irregular sampling rates. For example, probe vehicles upload their GPS data[1] with noise to the system with irregular sampling rates ranging from 15s to 120s. Therefore, it is possible that we do not have any data record for a certain time instant. To avoid this, we discretize the (within-day) time instant t to M time intervals T_m, the within-day process within each discretization interval is denoted as $\{X_{im} : m = 1, \cdots, M\}$. Day-to-day travel time process observed at time interval T_m is denoted by $\{X_m(i) : i = 1, \cdots, N\}$. Raw measurements are denoted as a matrix $\mathbf{V_m} = [\mathbf{V_{1m}}, \cdots, \mathbf{V_{Nm}}]^T$, where $\mathbf{V_{im}}$ is a vector of measurements observed in day i during time interval T_m, i.e., $\mathbf{V_{im}} = \{V_{im}(t_j) : t_j \in T_m, j = 1, \cdots, n_i\}$, with t_j the time instant that the data sample j is recorded.

2.1. Within-day travel time estimation

The within-day process $X_i(t)$ is assumed to follow a Gaussian process that it can be specified by its mean function $\mu_i(t) = E(X_i(t))$ and covariance function $G(t, s) = \text{cov}(X_i(t), X_i(s))$, respectively. Suppose $G(t, s) = \text{cov}(X_i(t), X_i(s))$, $\forall s,\ t$, has orthonormal expansions as follows:

$$G(t, s) = \sum_{k=1}^{\infty} \lambda_k \psi_k(t) \psi_k(s) \tag{1}$$

where $\{\lambda_k,\ \forall k\}$ is a set of eigenvalues in non-ascending order and $\{\psi_k\}$ is the corresponding set of eigenfunctions that form an orthonormal set of basis with a unit norm. According to the Karhunen-Loève representation, process $X_i(t)$ can be expanded as

$$X_i(t) = \mu(t) + \sum_{k=1}^{\infty} \xi_{ik} \psi_k(t) \tag{2}$$

[1] Although we mainly use GPS data of probe vehicles in this paper, the proposed methodology can be applied to other data sources as well.

where ξ_{ik} is a random coefficient (known as a functional principal component (FPC)), satisfying $E(\xi_{ik}) = 0$ and $var(\xi_{ik}) = \lambda_k$. The raw traffic data collected everyday can be regarded as discrete observations sampled from the within-day stochastic traffic process. Considering the data availability and the within-day time discretization T_m, the measurement $V_{im}(t_j)$ of the within-day travel time process as a function of time $t \in T_m$, i.e., $X_{im}(t)$, at sampling time $t_j,\ \forall t_j \in T_m$, is polluted by random noise e_{im}, we have

$$V_{im}(t_j) = X_{im}(t_j) + e_{im} = \mu(t_j) + \sum_{k=1}^{\infty} \xi_{ik}\psi_k(t_j) + e_{im},\ t_j \in T_m \tag{3}$$

where e_{im} are assumed to be uncorrelated with each other and are independent of ξ_{ik} with $E(e_{im}) = 0$, $\text{var}(e_{im}) = \omega^2$. This assumption is not strictly necessary if $\omega^2_{im} = \text{var}(e_{im})$ can be regarded as the discretization of a smooth variance function $\omega^2(t)$ such that $\omega^2_{im} = \omega^2(t_j)$.

The FDA is claimed to be a powerful tool for analyzing noisy data with irregular sample rates in the statistics literature (Yao et al., 2005; Wang et al., 2016). On the other hand, The FDA can act as a dictionary-based data compression method to identify the features of both spatial and temporal traffic patterns using the eigenfunctions extracted from the training data. Zhong et al. (2017) applied the FDA for within-day travel time prediction under abnormal traffic conditions and showed its computational efficiency for real-time applications. Therefore, we adopt the FDA to generate useful knowledge (or the set of eigenfunctions) of within-day travel time distributions of all sample days to reduce the "redundancy" of the raw data. The algorithm for estimating the within-day travel time process by the FDA is summarized in terms of Pseudocode as presented in Table 2.

In the FDA, the Karhunen-Loève decomposition is used for the eigenanalysis of general linear operators, which is essentially the singular value decomposition in the functional context. The functional principal component analysis (FPCA) can be regarded as an extension of the PCA for multivariate data to functional data. The underlying stochastic process $X_{im}(t)$ can be represented by a linear combination of a countable sequence of FPCs (or scores) $\xi_{ik}, k = 1, \cdots, \infty$, which are uncorrelated random variables, and the corresponding orthogonal eigenfunctions (i.e., the basis functions) $\psi_k(t),\ k = 1, \cdots, \infty$. In practice, the FPCs are truncated to a finite vector accomplishing the goal of dimension reduction. The FPCA "converts" the functional data (of infinite-dimension) to a vector of random scores of dimension K with each process represented by their vector of scores on this basis. Then the analysis concerning the resulting random vector of FPCs can be accomplished using the tools of multivariate statistical analysis.

2.2. Double time-scale model

Note that the within-day travel time processes are evaluated independently day by day. Real-time traffic condition disseminated through advanced traveler information systems (ATIS) in conjunction with travelers' day-to-day experience would affect their choices and thus will affect the day-to-day traffic evolution, which further complicates the travel time dynamics. How these two time-scale dynamics are coupled has been rarely modeled and explored in the literature. The Gaussian process is often used in the literature for capturing the day-to-day transient traffic phenomenon to steady-state traffic behavior (see e.g. Watling and Hazelton (2018) and the references therein) and also the within-day traffic dynamics (see e.g. Yeon et al. (2008); Zhong et al. (2017) and the references therein). As reviewed, Lognormal distribution is widely used to fit travel time distribution in the literature. The geometric Brownian motion (GBM)[2], which is a powerful tool in the stock pricing context, offers a bridge to connect these two observations. Moreover, the GBM is analytically tractable for modeling stochastic processes described by Lognormal distributions. Therefore, we proposed a modified GBM to model the double time-scale travel time process. On the other hand, as mentioned in the introduction, conventional day-to-day models cannot use the raw traffic data directly but have to aggregate the raw traffic data into a "point" for each day due to the within-day static traffic assumption. The FDA presented in the last section can take in raw traffic data to capture the variability of within-day travel time process and the effect of noise in traffic data. Inspired by the GBM model, the geometric transformation is adopted to transform the Gaussian within-day process into a Lognormal one, so as to capture the skewed distributions of travel time under

[2] The model of geometric Brownian motion is $dX_t(i) = \alpha_t X_t(i)di + \beta_t X_t(i)dB_i$ where α_t,β_t are the drift (trend) and volatility parameters of the stochastic process X_t and the Brownian motion (or Wiener process) $B_t \sim \mathbb{N}(0, t)$. The initial value of the Wiener process is $B_0 = 0$ yielding $X(0) = 1$.

Table 2: Within-day travel time estimation using functional data analysis.

Functional Data Analysis Algorithm in Pseudocode

Start

Input: Load data $\mathbf{V_m}$ (the input time grid could be irregular, i.e. $\{t_{ij} : i = 1, \cdots, N, j = 1, \cdots, n_i\}$);

Initialization:

Set the threshold $\kappa = 95\%$ for model selection.

Kernel type: Gaussian; Bandwidth selection: Generalized Cross-Validation (GCV)

(Mean function):

Apply locally weighted least square (LWLS) to scatterplots $\left\{(t_{ij}, V_m(t_{ij})) : i = 1, \cdots, N,\ j = 1, \cdots, n_i\right\}$:

$$\min_{\beta_0,\beta_1} \sum_{i=1}^{N}\sum_{j=1}^{n_i} K_1\left(\frac{t_{ij}-t}{h_\mu}\right)\{V_m(t_{ij}) - \beta_0 - \beta_1(t-t_{ij})\}^2$$

(K_1 is a univariate kernel function. h_μ is the bandwidth.)

$\Longrightarrow$ a smooth mean function $\hat{\mu}(t) = \hat{\beta}_0(t), t \in T_m$

(Covariance surface):

Apply two-dimensional LWLS to scatterplots $\left\{(t_{ij}, t_{il}), (V_m(t_{ij}) - \hat{\mu}(t_j))((V_m(t_{il}) - \hat{\mu}(t_l)) : i = 1, \cdots, N,\ j, l = 1, \cdots, n_i, j \neq l\right\}$:

$$\min_{\beta_0,\beta_{11},\beta_{12}} \sum_{i=1}^{N}\sum_{j=1,j\neq l}^{n_i} K_2\left(\frac{t_{ij}-t}{h_{C_1}}, \frac{t_{il}-s}{h_{C_2}}\right)\{(V_m(t_{ij}) - \hat{\mu}(t_j))((V_m(t_{il}) - \hat{\mu}(t_l)) - (\beta_0 + \beta_{11}(t-t_{ij}) + \beta_{12}(s-t_{il}))\}^2$$

(K_2 is a bivariate density. h_{C_1}, h_{C_2} are bandwidths.)

$\Longrightarrow$ a smooth covariance surface $\widehat{\text{cov}}(X_{im}(t), X_{im}(s)) = \hat{\beta}_0(t, s), t, s \in T_m$

(Principal components):

Spectral decomposition to covariance: $\text{cov}(X_{im}(t), X_{im}(s)) = \sum_{k=1}^{\infty} \lambda_k \psi_k(t)\psi_k(s)$

Discretizing $\widehat{\text{cov}}(X_{im}(t), X_{im}(s))$ in a regular output time grid;

Solve the eigenequations $\int_{T_m} \text{cov}(X_{im}(t), X_{im}(s))\ \psi_k(s)\,\mathrm{d}s = \lambda_k \psi_k(t)$;

Sort λ_k in descending order and rearrange k

$\Longrightarrow$ eigenvalues $\hat{\lambda}_k$ and eigenfunctions $\hat{\psi}_k(t)$

Determine the number of principal components K: (Take the fraction of variance explained (FVE) method as an example.)

Evaluate: FVE $= \sum_{k=1}^{K}(\hat{\lambda}_k)/\sum_{k=1}^{H}(\hat{\lambda}_k) > \kappa$, ($H$ is the number of $\hat{\lambda}_k$.)

$\Longrightarrow$ the number of principal components K

(Scores of principal components):

Apply principal analysis by conditional expectation (PACE):

$\hat{\xi}_{ik} = E(\hat{\xi}_{ik}|\mathbf{V_{im}}) = \hat{\lambda}_k \hat{\psi}_{ik}^T \hat{\Sigma}^{-1}_{\mathbf{V_{im}}}(\mathbf{V_{im}} - \hat{\mu}_{\mathbf{im}})$, where $\hat{\mu}_{\mathbf{im}} = (\hat{\mu}(t_1), \cdots, \hat{\mu}(t_{n_i}))^T$, $\hat{\Sigma}_{\mathbf{V_{im}}} = \widehat{\text{cov}}(V_m(t_{ij}), V_m(t_{il}))$

$\Longrightarrow$ scores $\{\hat{\xi}_{ik}\}$

Output:

$X_{im}(t) = \hat{\mu}(t) + \sum_{k=1}^{K} \hat{\xi}_{ik}\hat{\psi}_k(t) \Longrightarrow$ within-day travel time function $X_{im}(t), i = 1, \cdots, N, m = 1, \cdots, M$, whose mean and covariance functions are $\mu_{im}(t) = \hat{\mu}(t) + \sum_{k=1}^{K} \hat{\xi}_{ik}\hat{\psi}_k(t)$, $\sigma^2_{im}(t) = \sum_{k=1}^{K} \hat{\lambda}_k \hat{\psi}_k(t)\hat{\psi}_k(t)$, with $\hat{\lambda}_k = var(\hat{\xi}_{ik})$

End

abnormal traffic conditions. The double time-scale travel time process is modeled as:

$$\mathrm{d}X_m(i) = \alpha_m X_m(i)\mathrm{d}\mu_{im} + \beta_m X_m(i)\mathrm{d}\sigma_{im}\epsilon, \quad \epsilon \sim \mathbb{N}(0,1) \tag{4}$$

where α_m, β_m are drift and volatility parameters of the stochastic process X_m and μ_{im}, σ_{im} are the mean and standard deviation of X_{im} obtained from the FDA. The first component describes the day-to-day process under a risk-free condition, while the second component describes the uncertainties induced by external effects.

Let $F_m(i) = \log X_m(i)$, then we have

$$\mathrm{d}F_m(i) = \mathrm{d}\log X_m(i) = \frac{1}{X_m(i)}(\mathrm{d}X_m(i)) = \alpha_m \mathrm{d}\mu_{im} + \beta_m \mathrm{d}\sigma_{im}\epsilon \tag{5}$$

Note that the discrete-time nature of the day-to-day process and in line with Cantarella and Watling (2016), we use a difference version to replace the above differential process (in continuous-time) to yield a discrete-time day-to-day

process as:

$$\Delta \log X_m(i) = \log X_m(i) - \log X_m(i-1) = \log\left(\frac{X_m(i)}{X_m(i-1)}\right) \sim \mathcal{GP}\left(E[\Delta F_m(i)], D[\Delta F_m(i)]\right) \tag{6}$$

where $\mathcal{GP}(\cdot,\cdot)$ denotes the Gaussian process, $E[\Delta F_m(i)]$ and $D[\Delta F_m(i)]$ are the mean and variance of $\Delta F_m(i)$, respectively.

According to the properties of Lognormal distribution (Please kindly refer to the online appendix for details), we have

$$\begin{aligned} E\left[\tfrac{X_m(i)}{X_m(i-1)}\right] &= \exp\left(E[\Delta F_m(i)] + \tfrac{D[\Delta F_m(i)]}{2}\right) \\ D\left[\tfrac{X_m(i)}{X_m(i-1)}\right] &= E\left[\tfrac{X_m(i)}{X_m(i-1)}\right]^2 - \left(E\left[\tfrac{X_m(i)}{X_m(i-1)}\right]\right)^2 = \exp\left(2E[\Delta F_m(i)] + D[\Delta F_m(i)]\right)\left(\exp\left(D[\Delta F_m(i)]\right) - 1\right) \end{aligned} \tag{7}$$

for each day i. As the stochastic process X_m evolves from day to day, we could obtain the probability density function (PDF) of $X_m(i-1)$ by recursive iteration. Given a realization $\overline{X}_m(i-1)$ of $X_m(i-1)$, and its PDF $p(\overline{X}_m(i-1))$, we can derive the conditional mean and variance of $X_m(i)$ as:

$$\begin{aligned} E[X_m(i)|\overline{X}_m(i-1)] &= \overline{X}_m(i-1)\exp\left(E[\Delta F_m(i)] + \tfrac{D[\Delta F_m(i)]}{2}\right) \\ D[X_m(i)|\overline{X}_m(i-1)] &= \left(\overline{X}_m(i-1)\right)^2 \exp\left(2E[\Delta F_m(i)] + D[\Delta F_m(i)]\right)\left(\exp(D[\Delta F_m(i)]) - 1\right) \end{aligned} \tag{8}$$

$$E[X_m(i)] = \int E[X_m(i)|\overline{X}_m(i-1)]p(\overline{X}_m(i-1))\mathrm{d}\overline{X}_m(i-1)$$

According to the transformation of normal and Lognormal distributions, we take the medians as the realizations of day-to-day travel time under Lognormal assumptions while the mean values are for within-day travel time under Gaussian assumptions. Under this assumption, the realization of $X_m(i)$ is given by

$$\overline{X}_m(i) = \overline{X}_m(i-1)\exp\left(E[\Delta F_m(i)]\right), \tag{9}$$

where we have used median value of $X_m(i-1)$ to proceed the calculation that renders $D[\Delta F_m(i)]/2 = 0$.

Let $X_m(i) \sim \text{Lognormal}(a_{im}, b_{im}^2)$, then the parameters could be evaluated by

$$a_{im} = \ln\left(\frac{E[X_m(i)]}{\sqrt{1 + \frac{D[X_m(i)]}{(E[X_m(i)])^2}}}\right), \quad b_{im}^2 = \ln\left(1 + \frac{D[X_m(i)]}{(E[X_m(i)])^2}\right) \tag{10}$$

3. Model calibration

Model calibration can be regarded as an optimization problem.

$$u^* = \arg\min_{u \in U} S(F(u), O) \tag{11}$$

where $S(F(u), O)$ is the objective function that evaluates the difference between a model $F(u), u \in U$ output and its observation counterpart O. As the travel time distributions could be skewed under abnormal traffic conditions, it would be biased when one chooses to minimize the mean squared error. Thus, we introduce the relative entropy (also known as Kullback-Leibler (KL) divergence/distance) to measure the difference between the estimated distribution and the empirical distribution.

The relative entropy is often used to measure the dissimilarity of two probability distributions, e.g., $p(x)$ and $q(x)$. To be specific, the KL distance of q from p, denoted $D_{KL}(p||q)$, measures loss/change of information when $q(x)$ is used to approximate $p(x)$. For discrete probability distributions p_k and q_k, the KL distance of q from p is defined as

$$D_{\mathrm{KL}}(p||q) = \sum_{k=1}^{K} p_k \ln \frac{p_k}{q_k}$$

For continuous distributions $p(x)$ and $q(x)$, the KL distance is defined as:

$$D_{\mathrm{KL}}(p\|q) = \int_{-\infty}^{\infty} p(x)\ \ln \frac{p(x)}{q(x)}\,\mathrm{d}x$$

It can be shown that the KL distance is connected to the cross entropy $H(p,q)$ (for the distributions p and q) through the following relationship:

$$H(p,q) = H(p) + D_{\mathrm{KL}}(p\|q)$$

where $H(p)$ is the entropy of p, which is defined as

$$H(p) = -E(\ln(p)) = -\int p(x)\ln(p(x))dx$$

The objective function for calibrating the modified GBM is

$$\min_{\alpha_m,\beta_m} \frac{1}{N}\sum_{i=1}^{N} E_{p(\mathbf{V_{im}})}\left(\ln \frac{p(\mathbf{V_{im}})}{p(X_m(i);\alpha_m,\beta_m)}\right) + \frac{1}{N}\sum_{i=1}^{N}\left(\frac{\left|\overline{V}_{im} - \overline{X}_m(i)\right|}{\overline{V}_{im}}\right) \tag{12}$$

where the median $\overline{X}_m(i)$ (used to replace the mean for skewed distributions) and probability density function (PDF) $p(X_m(i);\alpha_m,\beta_m)$ are model outputs under parameters α_m,β_m. The first component in the objective function is the mean of relative entropy where $E_{p(\mathbf{V_{im}})}(\cdot)$ denotes the expectation under the PDF $p(\mathbf{V_{im}})$. The second component is a penalty term (a lasso-like regularization term) using the mean absolute percentage error (MAPE) (again using median rather than mean) to guarantee a small bias between the model realizations and empirical measurements.

For calibration purpose, we bin the irregular data samples of day i during time interval T_m to their mean value $\overline{V}_{im}$[3]. Stacking $\overline{V}_{im}$ yields a vector of day-to-day observations during time interval T_m as $\mathbf{W_m} = \left(\overline{V}_{1m},\cdots,\overline{V}_{Nm}\right)^T$. Considering the larger volatility of travel time under abnormal traffic conditions, we firstly group the sample days before calibration. The travel time patterns can be very different in regular and abnormal traffic conditions. The days separated into the same group will have similar travel time patterns so that the double time-scale travel time model for the days in each group is calibrated independently. The bounding boxes for data grouping are defined as:

$$2(r-1)\cdot\delta < \mathbf{W_m} - \min(\mathbf{W_m}) \le 2r\cdot\delta, r = 1,\cdots,R \tag{13}$$

where δ is the difference between the median value and minimum value of $\mathbf{W_m}$. As shown in Figure 3, the sample days are classified into R groups according to the deviation of realizations from the median value of empirical day-to-day distributions. Further, we apply a cross-entropy method (CEM) to search for the optimal solution following the model calibration method proposed by Zhong et al. (2016). Assume the unknown parameters following Gaussian distributions with large variance so as to cover a large enough sampling range, an importance sampling technique is adopted for effective and fast convergence. The model calibration algorithm is summarized in terms of pseudocode as presented in Table 3.

4. Empirical studies

In this section, we conducted two empirical studies with different network scales to validate the proposed model under different traffic scenarios, i.e., a long expressway in Guangzhou under traffic accidents and the urban network of New York City under Hurricane Sandy. Both case studies adopted probe vehicle data but with different configurations. The GPS data of the expressway case is for traffic monitoring purpose that contains the location of probe vehicles with sampling rates up to seconds. On the other hand, the taxi data of New York City is coarse in the sense that it contains only OD coordinates for each trip.

[3] The data grouping is inspired by the idea of data binning used in calibrating freeway fundamental diagrams when there is significant data scattering. The data is grouped because of the large volatility of travel time under abnormal traffic conditions. The travel time patterns can be very different under recurrent and abnormal traffic conditions (or day-of-the-week). To be specific, travel time under traffic disruptions would admit a sharp increase. In contrast, travel time is relatively stable and with small fluctuation under recurrent circumstances. To ensure the accuracy of calibration, the daily travel time profiles have similar patterns are grouped.

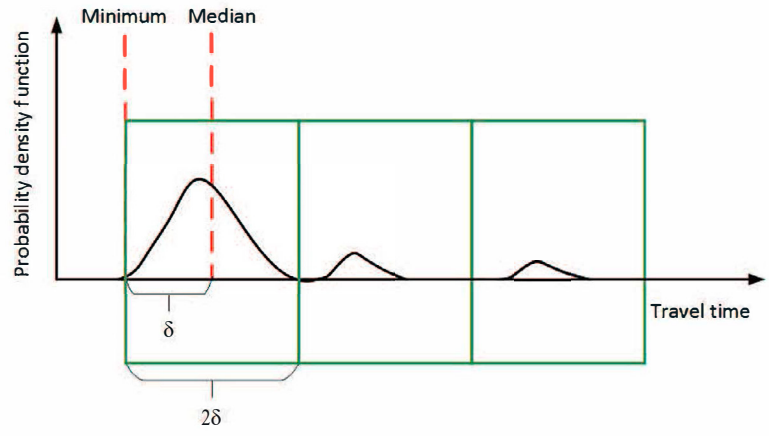

Fig. 3. Data grouping with a bounding box.

Table 3: Algorithm for model calibration.

Model Calibration Algorithm in Pseudocode

Start
Grouping: sample days are separated into R groups using bounding boxes
Initialization:
the sample size for the random sampling: ϕ_1; the sample size for the importance sampling: ϕ_2;
updating rate: ρ; threshold for convergence (a very small value): o;
parameters a_m^r, b_m^r follow Gaussian distributions with PDFs $f_0(a_m^r), g_0(b_m^r)$;
Initialize $r = 0$:
Do $r = r + 1$
Initialize $l = 0$:
Do $l = l + 1$
Random sampling: randomly sample from $f_{l-1}(a_m^r), g_{l-1}(b_m^r)$
$\Longrightarrow$ a series of parameter sets $\mathbf{u}_{\phi_1}$
Importance sampling:
evaluate the objective function;
sort the objective values in ascending order;
determine a small subset of "good" samples $\mathbf{u}_{\phi_2}$ that derive the smallest objective value;
$\Longrightarrow$ "good" samples $\mathbf{u}_{\phi_2}$
Update distribution:
new distribution: $\mathbf{u}_{\phi_2} \Longrightarrow f_l^{new}(\alpha_m^n), g_l^{new}(\beta_m^n)$
smooth updating law:
$f_l(a_m^r) = \rho f_{l-1}(a_m^r) + (1-\rho) f_l^{new}(a_m^r)$; $g_l(b_m^r) = \rho g_{l-1}(b_m^r) + (1-\rho) g_l^{new}(b_m^r)$
$\Longrightarrow$ updated distribution $f_l(a_m^r), g_l(b_m^r)$
Until parameters' standard deviations $\leq o$
Until $r = R$
End

4.1. Double time-scale travel time analysis for an expressway corridor under traffic accidents

To validate the effectiveness of the proposed model, we conducted a case study on the Guangzhou Airport South Expressway from Ping Sha to Airport South as shown in Figure 4. The expressway is of 16.693-km in length and is divided into 17 links of equal length (1 km) except for link 10, which is 693 m in length. Note that links 1, 2 and 14 are the weaving sections. This expressway has a monthly average daily traffic of over 50,000 vehicles, wherein the probe vehicles account for about 3.7%. One month GPS data of probe vehicles between March 1 and April 2 in 2014 was adopted in this empirical study. The dataset is extracted from the floating car trajectory data of the open data

program provided by the OpenITS project [4]. The sampling rate ranges from 15s to 120s. March 18 was excluded due to data incompleteness. Within this one-month study period, there were four traffic accidents as shown in Table 4. We chose the FVE to determine the best number of principal components and set the threshold as 0.95, which means the principal components should at least account for 95% travel time variation.

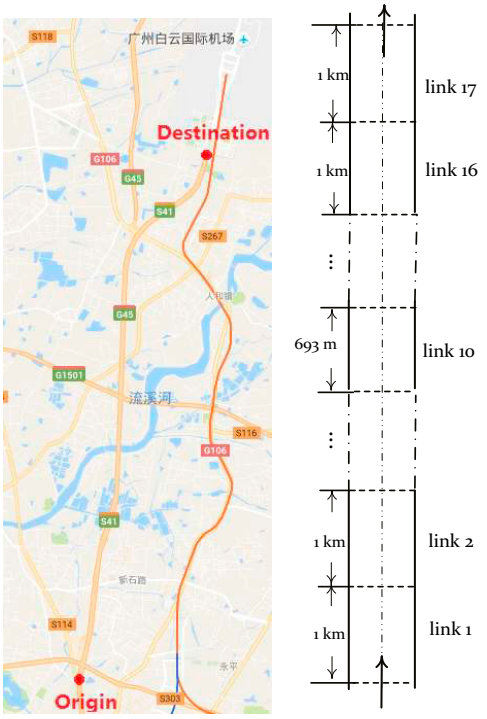

(a) Google map of the test site (b) Sketch map

Fig. 4. The segment of Guangzhou Airport Expressway under consideration. The origin and destination are marked to indicate the direction of traffic flow considered in this empirical study.

Firstly, the estimations of within-day travel time functions of four cases in line with the incident records are presented. From the results in Figure 5, two traffic accidents induced significant increases to link travel times. The FDA method is adaptive to the travel time patterns under abnormal traffic conditions including the congestion onset and offset. The FDA captures the variability of within-day travel time process and is robust to the noise in traffic data. It is also noted that the recorded time of traffic incidents in Table 4 is usually delayed when compared to the time that traffic states were affected by the incidents. Although the discrete samples from the estimated within-day travel time functions in accordance with the within-day time discretization T_m (the red circles) are close to the aggregated observations (the blue squares), the estimated travel time functions (the cyan lines) are insufficient to account for the travel time variability (the black dots). Therefore, we applied the proposed double time-scale model to derive both the within-day dynamics and the day-to-day dynamic travel time distributions.

The double time-scale travel time dynamics are shown in Figure 6. The within-day time instant was divided into time intervals every 5 minutes. To make the results more visible, logarithmic coordinates were used for drawing. The gray surface is the evolutionary process of the medians of the travel time dynamics produced by the proposed model

[4] The data can be downloaded from http://www.openits.cn/datadownload.php?dsid=2

Table 4: Incident records.

Date	Recorded time (24-hour clock)	Clearance time (24-hour clock)	Cause	Link
March 8, 2014	9:05	10:10	Loss of vehicle control	Link 6
March 23, 2014	13:17	14:20	Loss of vehicle control	Link 8
March 25, 2014	10:02	10:20	Rear-end collision	Link 3
April 2, 2014	12:00	12:24	Rear-end collision	Link 12

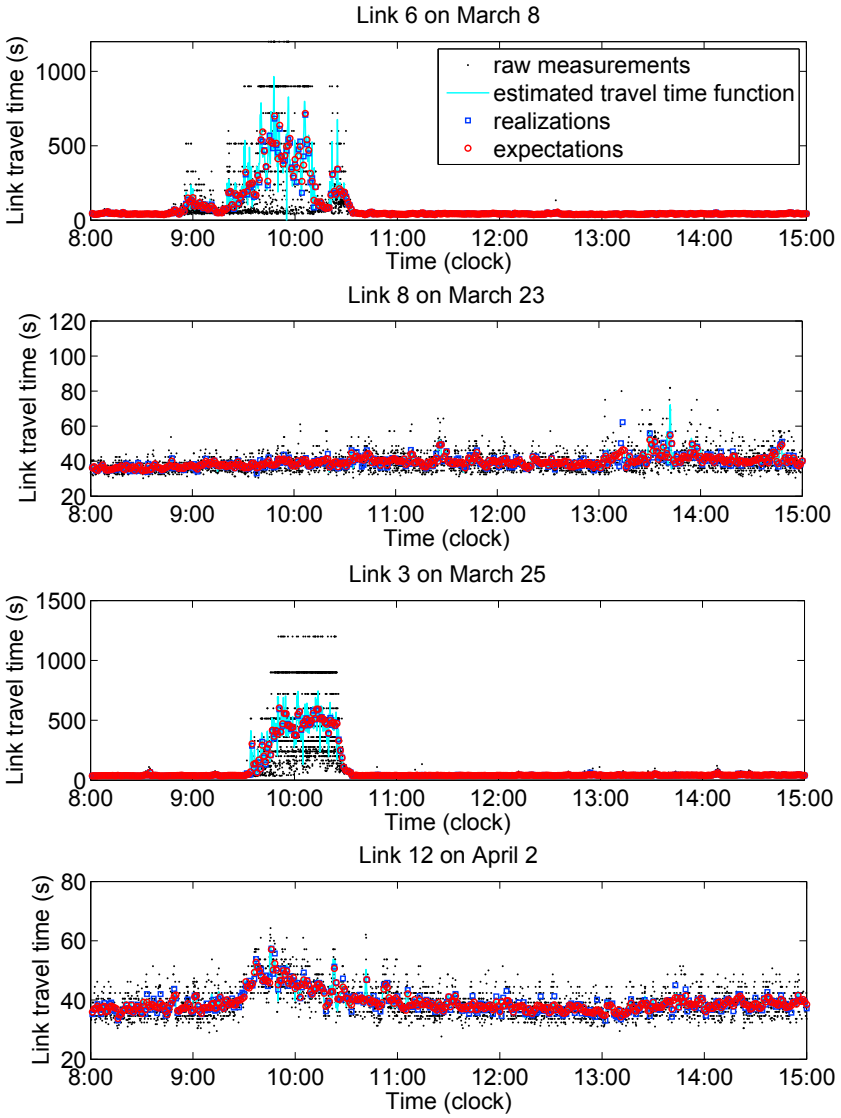

Fig. 5. The estimated within-day travel time functions and the measurements for four incident days.

against the measurement counterparts (i.e., the black dots). The pink and purple surfaces are the upper- and lower-bounds of travel time distributions accounting for 95% variability, i.e., the 95% confidence intervals. Taking one of the cross sections as an example, Figure 7 presents the day-to-day travel time process in 10:00-10:05 AM along with the within-day uncertainties. As shown in the figure, the proposed double time-scale travel time process can describe

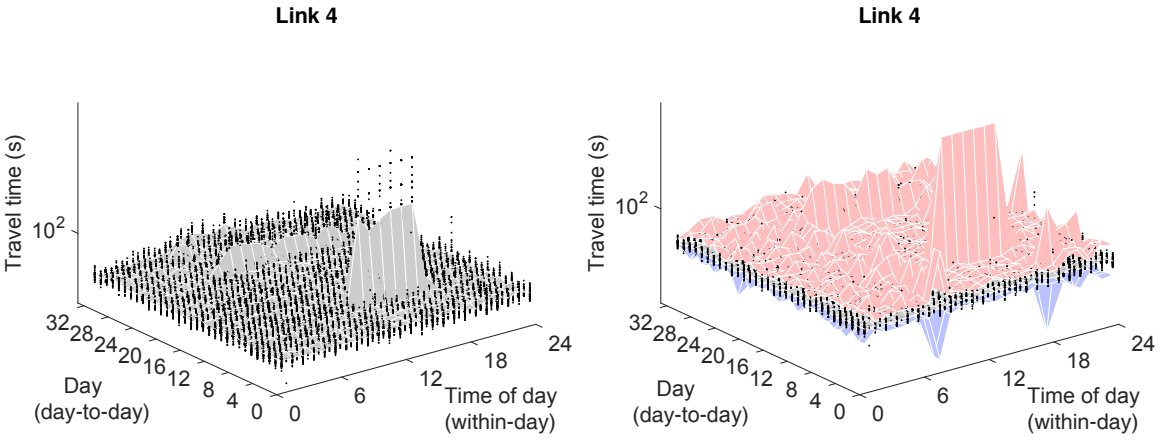

Fig. 6. 3D visualization of double time-scale travel time process.

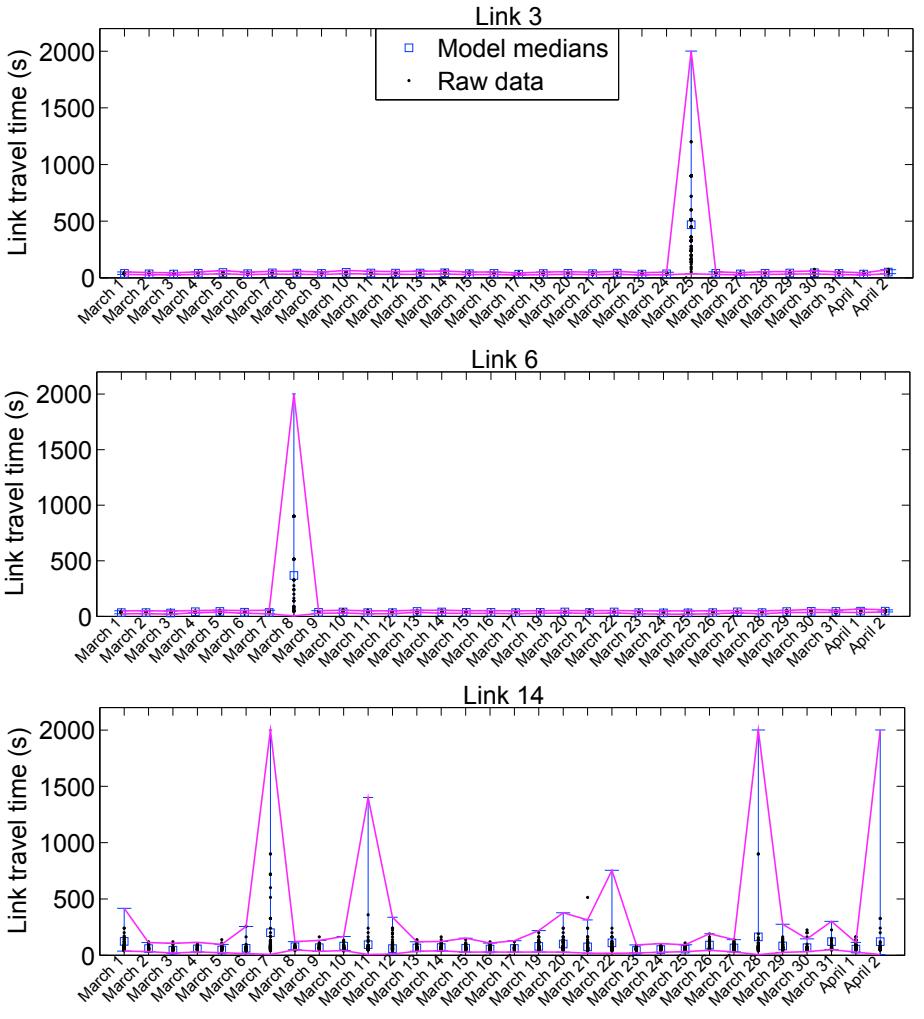

Fig. 7. Double time-scale travel time processes in 10:00-10:05 AM with 95% confidence level.

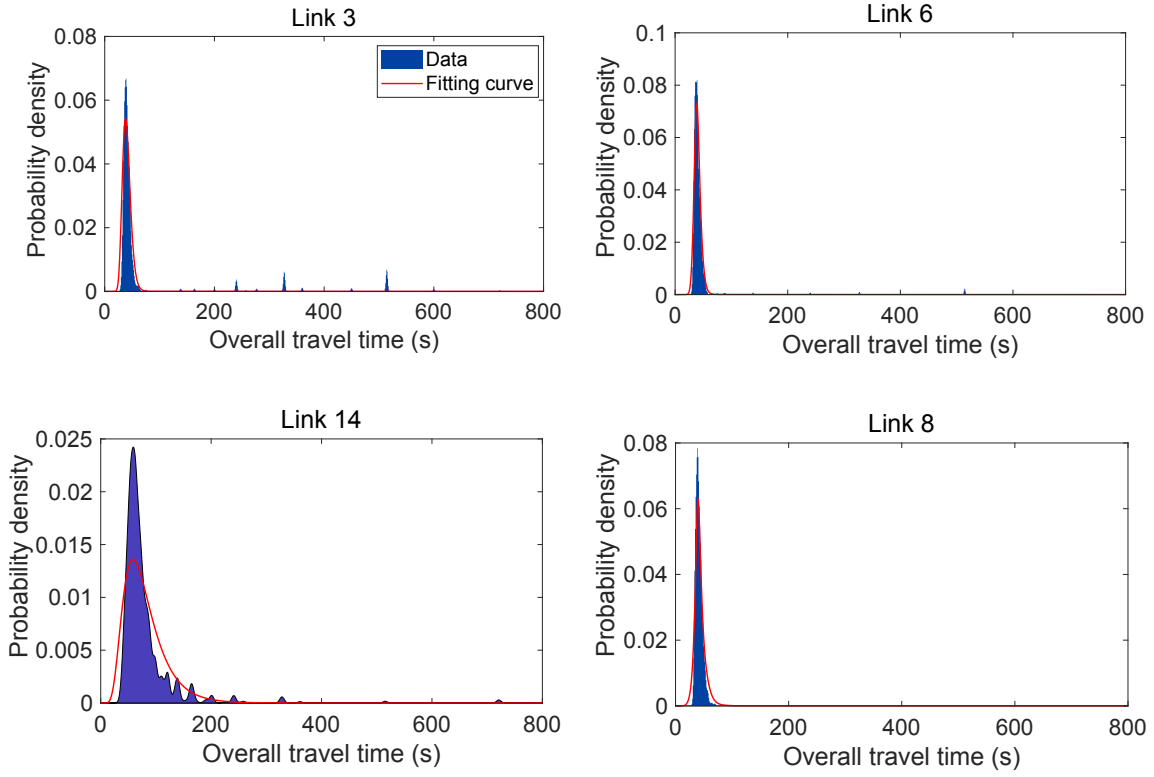

Fig. 8. Overall travel time distributions in 10:00-10:05 AM.

the variability of the day-to-day evolution of travel time from the transient impact caused by the traffic accidents to the normal steady state. The freeway traffic recovered to recurrent states within a day under these accidents. The impact of the weaving section in link 14 on the traffic states could be identified by high fluctuations of travel time. Moreover, Figure 8 depicts the mixture distributions that represent the probability distributions of the overall travel time. Irregular traffic incidents would lead to heavy tails on the right side of travel time distributions, whereas recurrent fluctuations would induce a skewed distribution.

In order to quantify the accuracy of these processes, two indices[5] were evaluated, i.e., the relative entropy between the estimated travel time distributions and the distributions derived from the raw data, and the proportion of inclusions, i.e., the ratio of raw measurements within the upper and lower bounds of the estimation to the total measurements. From the results in Table 5, we found that the proposed model could yield small values of relative entropy and large enough proportion of inclusions with 95% confidence level, which indicates reliable probability distributions.

The KL distance is small indicating good performance in terms of data and distribution fitting. The proportion of inclusions indicates the proposed model estimates the uncertainty in a satisfactory manner. This can also be observed from the distribution fitting process as indicated in Figure 8.

4.2. Double time-scale travel time analysis for an urban network under hurricane

In this example, we applied the proposed method to study the impacts of Hurricane Sandy on a large-scale traffic network with New York City taxi data[6]. The dataset includes four years of operation and details of nearly 700 million

[5] These indices are presented in the online appendix due to the page limit.
[6] This dataset is an open dataset available at http://dx.doi.org/10.13012/J8PN93H8.

Table 5: Performance of the double time-scale model for the expressway case.

Link	KL distance	Proportion of inclusions(%)	Link	KL distance	Proportion of inclusions(%)
1	0.1081	98.41	10	0.0876	94.92
2	0.0520	93.05	11	0.1102	95.22
3	0.2881	97.58	12	0.0722	94.02
4	0.1666	98.49	13	0.1324	93.80
5	0.2622	98.55	14	0.1927	97.45
6	0.1243	97.08	15	0.0826	84.75
7	0.0770	91.44	16	0.0706	92.94
8	0.0690	92.29	17	0.0357	93.04
9	0.1222	91.34			

trips of yellow taxi trips in New York City between 2010 and 2013. The data is organized by month, and each row represents a completed taxi trip. A sample of the raw trip data is shown in Table 6. It contains: pickup and dropoff times (start and end time of the trip), pickup longitude and pickup latitude (GPS coordinates at the origin of the trip) and dropoff longitude and dropoff latitude (GPS coordinates at the destination of the trip), trip duration (trip time measured by the taximeter in seconds) and trip distance (trip distance measured by the taximeter in miles). This dataset is regarded as coarse in the sense that it contains only two coordinates for each trip. The quality is lower than GPS data collected for traffic monitoring purpose such as that in the previous empirical study, which contains the location of vehicles with sampling rates up to seconds. However, it is still possible to analyze the city-scale resilience of the traffic conditions by the proposed method.

Table 6: A sample of raw data.

medallion	hack license	vendor id	rate code	store_and fwd_flag	pickup datetime	dropoff datetime	passenger count	trip_time in_secs	trip distance	pickup longitude	pickup latitude	dropoff longitude	dropoff latitude
2012000001	2012000001	CMT	1	N	2012/1/1 0:00:01	2012/1/1 0:05:49	1	348	1.2	-73.988945	40.726818	-74.004524	40.721397
2012005187	2012015775	CMT	1	N	2012/1/2 8:49:02	2012/1/2 8:57:20	1	497	3	-73.954659	40.780872	-73.978546	40.756702
2012008703	2012012505	VTS	2		2012/1/2 8:50:00	2012/1/2 9:17:00	2	1620	14.99	-73.815254	40.700146	-74.009247	40.738762
2012006692	2012010162	VTS	4		2012/1/2 13:19:00	2012/1/2 13:29:00	5	600	2.11	-73.952942	40.776421	-73.978241	40.764828
2012006280	2012024293	VTS	1		2012/1/3 22:35:00	2012/1/3 22:45:00	1	600	1.64	-73.981468	40.746417	-73.983841	40.760818

Following Donovan and Work (2017), the New York City was partitioned into four regions: East of the Hudson River (E), Upper Manhattan (U), Midtown (M), and Lower Manhattan (L), as demonstrated in Figure 9. To our purpose, we selected 47 days from October 15, 2012, to November 30, 2012, covering the periods before, during and after the Hurricane Sandy that hit New York City on October 29, flooding streets, tunnels and subway lines and cutting power in and around the city. We grouped the origins and destinations of trips by regions via matching their latitudes and longitudes. The trips were categorized into 16 travel types according to their OD pairs as shown in Table 7. In this study, we defined the pace as the normalized travel time, i.e., the ratio of trip travel time to trip distance. Discarding unreasonable trip records (accounting for about 8% of the records), we then evaluated the pace of each trip. In addition, there were much fewer trips during the period from October 29 and November 2 under the influence of the Hurricane Sandy. After applying the proposed method to derive the double time-scale pace (normalized travel time) processes, the model performance is presented in Table 8 using the two indices as previously explained. The KL distance is small indicating good performance in terms of data and distribution fitting for the New York case. The proportion of inclusions indicates the proposed model well estimates the uncertainty.

Figure 10 illustrates two examples of the double time-scale pace process in 3D visualization. A time increment of one hour was used to discretize the within-day time horizon. As indicated in Figure 10, compared with that of trip type 16 (trips from Lower Manhattan to Lower Manhattan), a larger variation of the pace of trip type 4 (trips from East of the Hudson River to Lower Manhattan) can be observed. Intuitively, trip type 4 is more susceptible to the Hurricane Sandy than trip type 16 as the trip crosses the harbor. On the other hand, trip type 16 has larger

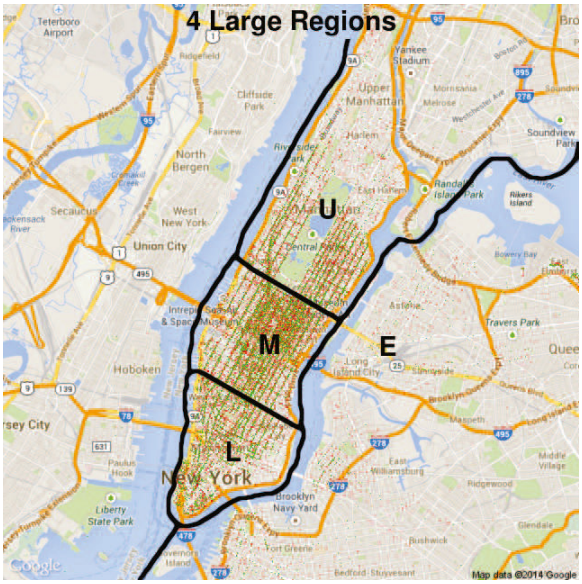

Fig. 9. The New York City network is partitioned into four regions denoted as East of the Hudson River (E), Upper Manhattan (U), Midtown (M), and Lower Manhattan (L) in line with Donovan and Work (2017).

Table 7: Trip types.

Pickup_region	E	E	E	E	U	U	U	U	M	M	M	M	L	L	L	L
Dropoff_region	E	U	M	L	E	U	M	L	E	U	M	L	E	U	M	L
Trip_type	E-E 1	E-U 2	E-M 3	E-L 4	U-E 5	U-U 6	U-M 7	U-L 8	M-E 9	M-U 10	M-M 11	M-L 12	L-E 13	L-U 14	L-M 15	L-L 16

Table 8: Performance of the double time-scale model for the New York case.

Type	KL distance	Proportion of inclusions(%)	Type	KL distance	Proportion of inclusions(%)
1	0.0757	98.10	9	0.0961	96.01
2	0.0899	96.62	10	0.0616	86.53
3	0.0532	86.40	11	0.0842	86.74
4	0.1614	87.26	12	0.0639	97.36
5	0.1021	96.95	13	0.1065	98.80
6	0.0474	95.89	14	0.1220	97.87
7	0.0794	86.82	15	0.0814	96.33
8	0.0653	92.33	16	0.0650	96.25

uncertainty under recurrent traffic conditions as Lower Manhattan is the central borough for business and finance. To observe the impact of the Hurricane Sandy on the pace evolution under day-to-day time-scale, we selected the time interval 12:00-13:00 (off-peak hour) to separate the congestion impact of the rush hours. As depicted in Figure 11, the day-to-day pace process of trip type 4 indicates that the disruption caused by the Hurricane Sandy lasted for several days since the statewide state of emergency was declared on 26 October till 5 November (3 days after it was

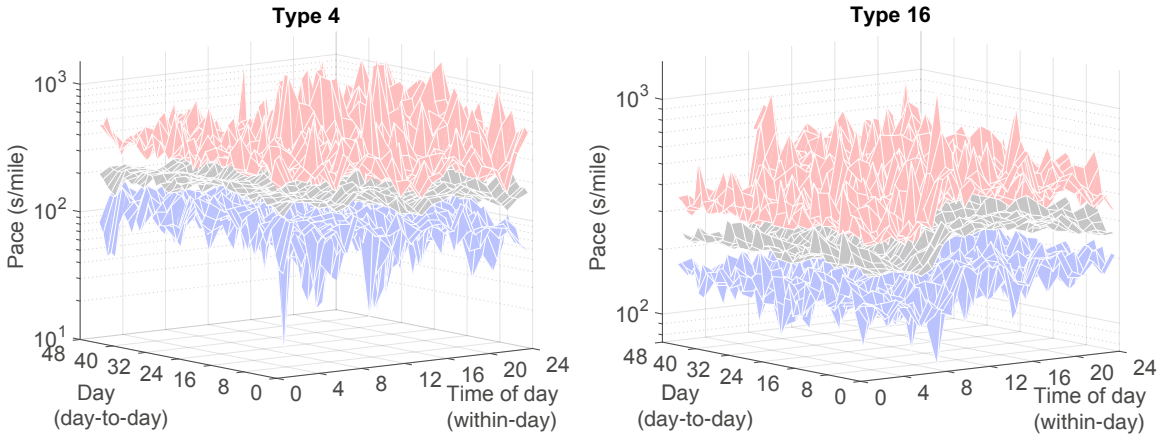

Fig. 10. 3D visualization of double time-scale pace process of trip type 4 and trip type 16.

Table 9: Impact of Hurricane Sandy on different trip types.

Type	1	2	3	4	5	6	7	8
Importance	0.0205	0.0162	0.0197	0.6973	0.0206	0.0206	0.0370	0.0209
Type	9	10	11	12	13	14	15	16
Importance	0.0232	0.0200	0.0094	0.0205	0.0125	0.0212	0.0198	0.0206

dissipated). The system gradually recovered to the recurrent traffic conditions. As shown in the probabilistic day-to-day evolution of travel time, the travel time distributions of these days are much wider than those of normal days. The travel time distributions of trip type 4 are spike during time interval 12:00-13:00 under recurrent traffic conditions indicating the travel time is reliable during off-peak hours. On the other hand, trip type 16 (trips within the CBD) under recurrent traffic conditions tends to admit a wide travel time distribution due to the heavy traffic in the CBD, while the rare events (e.g., Hurricane Sandy in this experiment) would lead to heavy tail on the right side of the pace distribution. The proposed double time-scale travel time model can provide reliable probabilistic distribution of the pace and can describe the variability of the pace, which allows the analysis on the short-term to long-term impacts of traffic disruptions on the performance of transportation systems.

4.2.1. Resilience analysis

Based on the overall pace distributions of all trip types, we quantify the importance of each trip type by estimating the weights of each trip type contributing to the network performance. Given D trip types, denote $R_m(i)$ as the network-scale pace distribution and $X_m^d(i)$ as the pace distribution of trip type $d = 1, \cdots, D$ in the time interval T_m of day i. The following optimization problem is to determine the importance for each type of trips on the network performance:

$$\min_{a^d} \sum_{i=1}^{N} \sum_{m=1}^{M} \left(\mathrm{E}\left[R_m(i) - \sum_{d=1}^{D} a^d \cdot X_m^d(i) \right] \right)^2 \tag{14}$$

where $0 \le a^d \le 1$, $\sum_{d=1}^{D} a^d = 1$ is the importance weighting of trip type d. By solving this problem, the results of trip importance are reported in Table 9. It is found that trip type 4 (E-M) contributes the most substantial impact on the network performance.

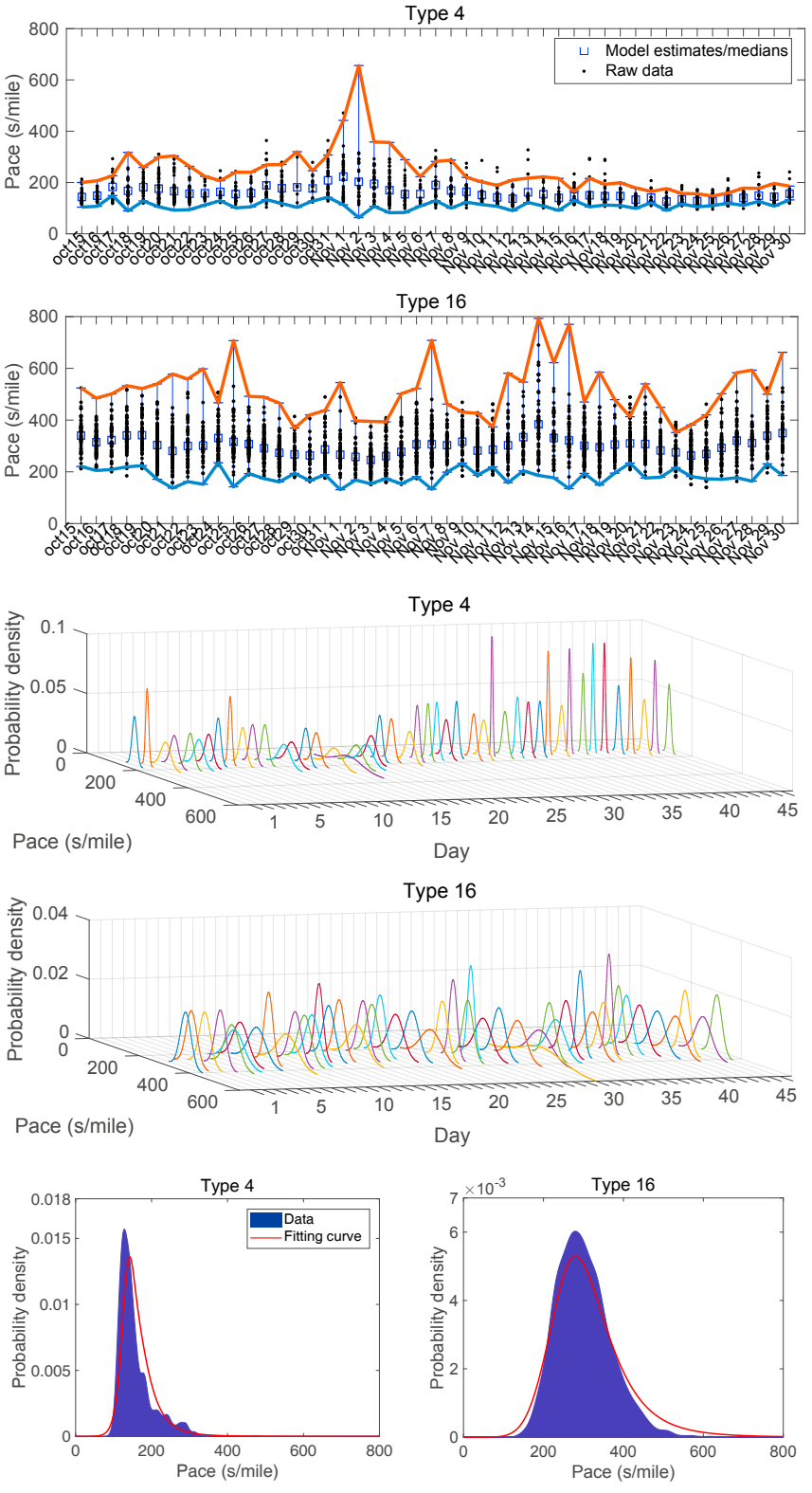

Fig. 11. Double time-scale pace process with 95% confidence levels, the probabilistic day-to-day evolution of travel time, and the overall travel time distribution fitting in the model calibration process for time interval 12:00 AM - 13:00 PM of trip type 4 and trip type 16.

5. Conclusion

This study integrated the data-driven and model-driven approaches to develop a double time-scale travel time model to probabilistically capture the day-to-day evolution along with the within-day variability of travel time. The proposed model extends the conventional day-to-day traffic models in the sense that the data-driven within-day process by the FDA enables direct input of raw traffic data with dynamic and noisy nature reflecting the effects of traffic congestion and external uncertainties. The within-day process was then regarded as the local volatility to drive the model-driven day-to-day process described by a modified geometric Brownian motion (GBM). The proposed double time-scale travel time model can describe the variability of the day-to-day evolution from the transient impact to the steady-state behavior (if any) of traffic disruptions and systematic changes, e.g., bridge collapse, hurricane, and new traffic policy measures, on the performance of traffic networks. Meanwhile, the proposed model can capture the variability of within-day travel time process and the effect of noise in traffic data. A relative entropy-based method was proposed for calibrating the double time-scale model, leading to proper distributions of interest. A lasso-like regularization was employed to guarantee a small bias between the model estimations and the measurement counterparts. A risk-based measure that adapts the heavy-tailed distribution of travel time was introduced to quantify the deterioration of network performance.

Two empirical studies at different scales, from long expressway corridor to a city-scale network, under different traffic scenarios, from traffic accidents to natural disaster, were conducted to validate the proposed model. As shown in the empirical studies, the FDA can handle the noisy and irregular sampling nature of probe vehicle data while considering the abnormal traffic conditions. The proposed model can capture the heavy tail characteristics of the travel time under rare events. The model is robust to different data configurations from coarse to fine, and small to big data. The proposed method can accommodate the inherent variability in traffic conditions and data meanwhile being computationally tractable.

Acknowledgements

The work in this paper was jointly supported by research grants from the Research Grants Council of the Hong Kong Special Administrative Region (Project No. 15210117 & 152628/16E), the Research Committee of the Hong Kong Polytechnic University (Project No. 1-BBAR) and the National Natural Science Foundation of China under Grant No. U1811463.

References

Al-Deek, H., Emam, E.B., 2006. New methodology for estimating reliability in transportation networks with degraded link capacities. Journal of intelligent transportation systems 10, 117–129.

Cantarella, G.E., Watling, D.P., 2016. A general stochastic process for day-to-day dynamic traffic assignment: Formulation, asymptotic behaviour, and stability analysis. Transportation Research Part B 92, 3–21.

Cascetta, E., Cantarella, G.E., 1991. A day-to-day and within-day dynamic stochastic assignment model. Transportation Research Part A 25, 277–291.

Chow, A.H., 2009. Properties of system optimal traffic assignment with departure time choice and its solution method. Transportation Research Part B 43, 325–344.

Crawford, F., Watling, D., Connors, R., 2017. A statistical method for estimating predictable differences between daily traffic flow profiles. Transportation Research Part B 95, 196–213.

Donovan, B., Work, D.B., 2017. Empirically quantifying city-scale transportation system resilience to extreme events. Transportation Research Part C 79, 333–346.

Fosgerau, M., Fukuda, D., 2012. Valuing travel time variability: Characteristics of the travel time distribution on an urban road. Transportation Research Part C 24, 83–101.

Friesz, T.L., Bernstein, D., Mehta, N.J., Tobin, R.L., Ganjalizadeh, S., 1994. Day-to-day dynamic network disequilibria and idealized traveler information systems. Operations Research 42, 1120–1136.

Friesz, T.L., Bernstein, D., Smith, T.E., Tobin, R.L., Wie, B.W., 1993. A variational inequality formulation of the dynamic network user equilibrium problem. Operations Research 41, 179–191.

Friesz, T.L., Bernstein, D., Stough, R., 1996. Dynamic systems, variational inequalities and control theoretic models for predicting time-varying urban network flows. Transportation Science 30, 14–31.

Friesz, T.L., Kim, T., Kwon, C., Rigdon, M.A., 2011. Approximate network loading and dual-time-scale dynamic user equilibrium. Transportation Research Part B 45, 176–207.
Guardiola, I.G., Leon, T., Mallor, F., 2014. A functional approach to monitor and recognize patterns of daily traffic profiles. Transportation Research Part B 65, 119–136.
Guo, R., Yang, H., Huang, H., Tan, Z., 2015. Link-based day-to-day network traffic dynamics and equilibria. Transportation Research Part B 71, 248–260.
Guo, R.Y., Yang, H., Huang, H.J., 2018. Are we really solving the dynamic traffic equilibrium problem with a departure time choice? Transportation Science 52, 603–620.
He, X., Liu, H., 2012. Modeling the day-to-day traffic evolution process after an unexpected network disruption. Transportation Research Part B 46, 50–71.
He, Y., He, J., Zhu, D., Zhou, J., 2010. Traffic network equilibrium with capacity constraints and generalized wardrop equilibrium. Nonlinear Analysis Real World Applications 11, 4248–4253.
Kim, J., 2014. Travel Time Reliability of Traffic Networks: Characterization, Modeling and Scenario-based Simulation. Ph.D. thesis. Northwestern University.
Kim, J., Mahmassani, H.S., 2015. Compound gamma representation for modeling travel time variability in a traffic network. Transportation Research Part B 80, 40–63.
Liu, W., Geroliminis, N., 2017. Doubly dynamics for multi-modal networks with park-and-ride and adaptive pricing. Transportation Research Part B 102, 162–179.
Liu, W., Li, X., Zhang, F., Yang, H., 2017. Interactive travel choices and traffic forecast in a doubly dynamical system with user inertia and information provision. Transportation Research Part C 85, 711–731.
Nagurney, A., Zhang, D., 1997. Projected dynamical systems in the formulation, stability analysis, and computation of fixed-demand traffic network equilibria. Transportation Science 31, 147–158.
Sandholm, W., 2010. Population Games and Evolutionary Dynamics. MIT Press.
Smith, M., 1984. The stability of a dynamic model of traffic assignment—an application of a method of lyapunov. Transportation Science 18, 245–252.
Sumalee, A., Pan, T., Zhong, R., Uno, N., Indra-Payoong, N., 2013. Dynamic stochastic journey time estimation and reliability analysis using stochastic cell transmission model: Algorithm and case studies. Transportation Research Part C 35, 263–285.
Taylor, M.A., 2013. Travel through time: the story of research on travel time reliability. Transportmetrica B 1, 174–194.
Wang, J.L., Chiou, J.M., Müller, H.G., 2016. Functional data analysis. Annual Review of Statistics and Its Application 3, 257–295.
Watling, D.P., Hazelton, M.L., 2018. Asymptotic approximations of transient behaviour for day-to-day traffic models. Transportation Research Part B 118, 90–105.
Yao, F., Müller, H.G., Wang, J.L., 2005. Functional data analysis for sparse longitudinal data. Journal of the American Statistical Association 100, 577–590.
Yeon, J., Elefteriadou, L., Lawphongpanich, S., 2008. Travel time estimation on a freeway using discrete time markov chains. Transportation Research Part B 42, 325–338.
Yildirimoglu, M., Limniati, Y., Geroliminis, N., 2015. Investigating empirical implications of hysteresis in day-to-day travel time variability. Transportation Research Part C 55, 340–350.
Zhong, R., Fu, K., Sumalee, A., Ngoduy, D., Lam, W.H.K., 2016. A cross-entropy method and probabilistic sensitivity analysis framework for calibrating microscopic traffic models. Transportation Research Part C 63, 147–169.
Zhong, R., Luo, J., Cai, H., Sumalee, A., Yuan, F., Chow, A.H.F., 2017. Forecasting journey time distribution with consideration to abnormal traffic conditions. Transportation Research Part C 85, 292–311.
Zhong, R., Sumalee, A., Friesz, T., Lam, W.H., 2011. Dynamic user equilibrium with side constraints for a traffic network: theoretical development and numerical solution algorithm. Transportation Research Part B 45, 1035–1061.
Zhong, R., Sumalee, A., Maruyama, T., 2012. Dynamic marginal cost, access control, and pollution charge: a comparison of bottleneck and whole link models. Journal of Advanced Transportation 46, 191–221.